Journal of Medicinal Chemistry

pubs.acs.org/jmc

Article

Ifenprodil Stereoisomers: Synthesis, Absolute Configuration, and Correlation with Biological Activity

Elena Bechthold, Julian A. Schreiber, Kirstin Lehmkuhl, Bastian Frehland, Dirk Schepmann, Freddy A. Bernal, Constantin Daniliuc, Inés Álvarez, Cristina Val Garcia, Thomas J. Schmidt, Guiscard Seebohm, and Bernhard Wünsch*

Cite This: J. Med. Chem. 2021, 64, 1170−1179

Read Online

ACCESS | Metrics & More | Article Recommendations | Supporting Information

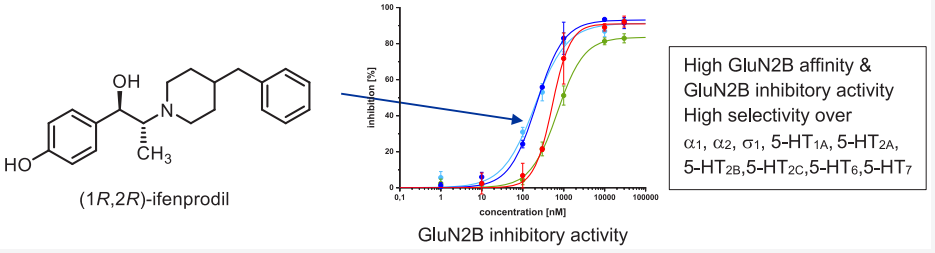

ABSTRACT: Ifenprodil (**1**) is a potent GluN2B-selective *N*-methyl-D-aspartate (NMDA) receptor antagonist that is used as a cerebral vasodilator and has been examined in clinical trials for the treatment of drug addiction, idiopathic pulmonary fibrosis, and COVID-19. To correlate biological data with configuration, all four ifenprodil stereoisomers were prepared by diastereoselective reduction and subsequent separation of enantiomers by chiral HPLC. The absolute configuration of ifenprodil stereoisomers was determined by X-ray crystal structure analysis of (1*R*,2*S*)-**1a** and (1*S*,2*S*)-**1d**. GluN2B affinity, ion channel inhibitory activity, and selectivity over α, σ, and 5-HT receptors were evaluated. (1*R*,2*R*)-Ifenprodil ((1*R*,2*R*)-**1c**) showed the highest affinity toward GluN2B-NMDA receptors (K_i = 5.8 nM) and high inhibition of ion flux in two-electrode voltage clamp experiments (IC_{50} = 223 nM). Whereas the configuration did not influence considerably the GluN2B-NMDA receptor binding, (1*R*)-configuration is crucial for elevated inhibitory activity. (1*R*,2*R*)-Configured ifenprodil (1*R*,2*R*)-**1c** exhibited high selectivity for GluN2B-NMDA receptors over adrenergic, serotonergic, and σ_1 receptors.

1. INTRODUCTION

The *N*-methyl-D-aspartate (NMDA) receptor plays a key role in excitatory neurotransmission in the mammalian brain.[1] It is a hetero-tetrameric protein complex that belongs to the family of ionotropic glutamate receptors.[2] The NMDA receptor contributes to long-term potentiation (LTP), a special form of synaptic plasticity, and is involved in brain functions such as learning and memory. Depolarization of the cell membrane combined with simultaneous binding of (*S*)-glutamate and glycine results in opening of the ion channel and influx of Ca^{2+} and Na^+ ions as well as efflux of K^+ ions.

Overstimulation of NMDA receptors leads to excessive influx of Ca^{2+} ions and subsequent cell death via apoptosis. This pathophysiological process termed excitotoxicity is involved in a variety of acute (e.g., stroke) and chronic (e.g., Parkinson's disease, Alzheimer's disease, Huntington's disease) neurological disorders.[3−5]

Seven genes encode different subunits, which are able to form the individual hetero-tetrameric ion channel receptor. The GluN1 subunit is encoded by a single gene, but post-translational modifications lead to eight splice variants termed GluN1a-h.[6,7] The four GluN2 subunits GluN2A−GluN2D are encoded by four different genes and show different expression levels throughout the central nervous system.[8] The residual genes encode the remaining GluN3A and GluN3B subunits. In general, a functional NMDA receptor contains two GluN1 and two GluN2 subunits, and the GluN3 subunits are expressed predominantly during the prenatal phase.[9] The channel properties and characteristics as well as their association with different diseases are mainly driven by the expressed GluN2 subunits.[10]

NMDA receptor antagonists that selectively target the GluN2B subunit are promising drug candidates for the treatment of neurodegenerative diseases due to less side effects compared to nonselective open-channel blockers such as ketamine or phencyclidine.[11]

Received: November 4, 2020
Published: January 11, 2021

https://dx.doi.org/10.1021/acs.jmedchem.0c01912
J. Med. Chem. 2021, 64, 1170−1179

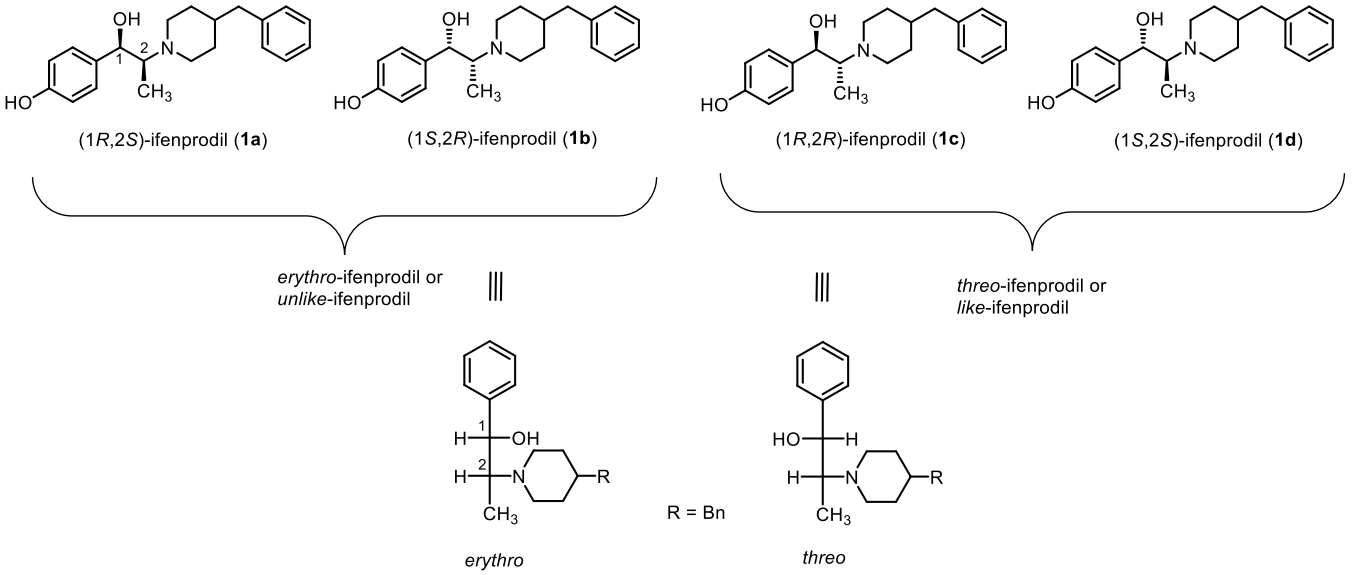

Figure 1. Ifenprodil stereoisomers.

Scheme 1. Synthesis of Ifenprodil Stereoisomers[a]

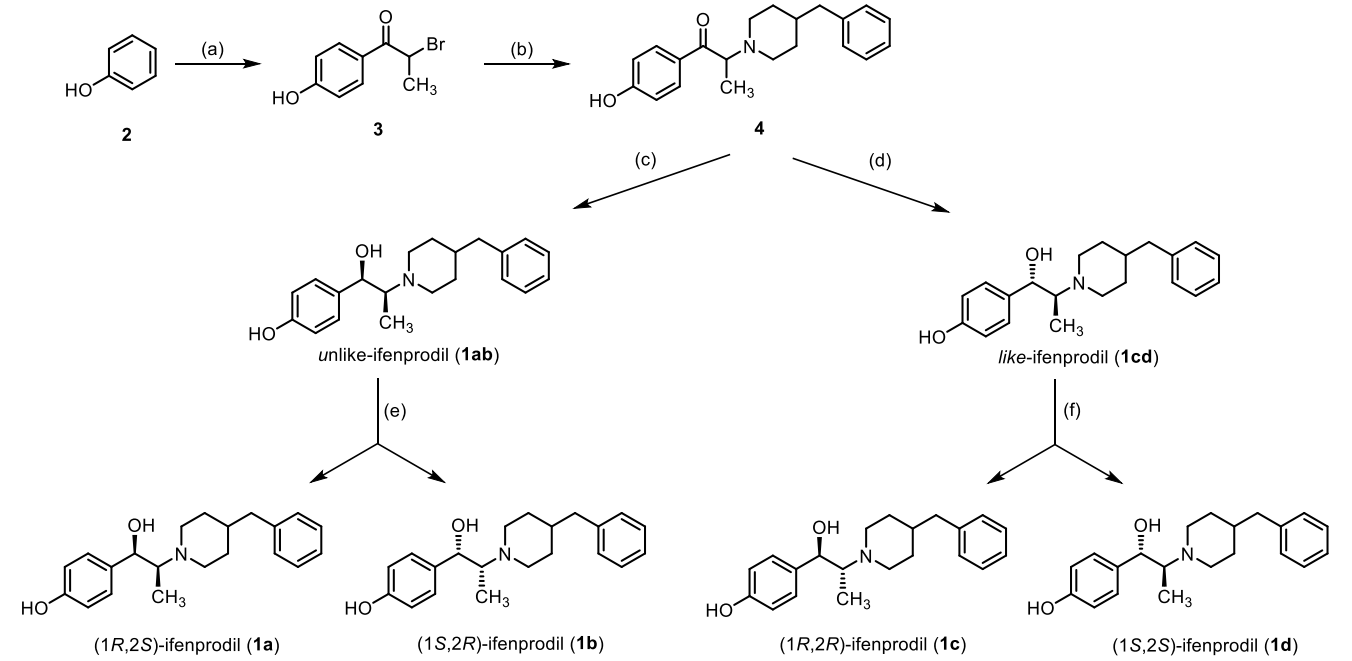

[a]Reagents and reaction conditions: (a) 2-bromopropionyl bromide, TfOH, neat, 0 °C, 5 min, then rt, 1 h, 69%. (b) 4-Benzylpiperidine, NEt_3, CH_2Cl_2, rt, 24 h, 86%. (c) KBH_4, HOAc, EtOH, 0 °C to rt, 16 h, 65%. (d) $LiAlH_4$, THF, −78 °C to rt, 16 h, 87%. (e) chiral HPLC: Daicel Chiralpak IA, 5 μm, 250 mm/20 mm; flow rate: 0−0.5 min 5 mL/min, 0.5−130 min 15 mL/min; injection volume: 400 μL (isohexane/iPrOH); detection λ = 275 nm; eluent: isohexane/iPrOH/MeOH = 93/5/2 + 0.1% Et_2NH. (f) chiral HPLC: Daicel Chiralpak IA, 5 μm, 250 mm/20 mm; flow rate: 0−0.5 min 5 mL/min, 0.5−130 min 15 mL/min; injection volume: 400 μL (isohexane/MeOH); detection λ = 275 nm; eluent: isohexane/MeOH = 97/3 + 0.1% Et_2NH.

Ifenprodil possesses two centers of chirality leading to four possible stereoisomers. The Fischer projection visualizes the stereodescriptors *erythro* and *threo*. Stereoisomers with the same or different stereodescriptors for the two centers of chirality are termed *like* (*l*) and *unlike* (*u*), respectively.[12]

In the literature, 2-(4-benzylpiperidin-1-yl)-1-(4-hydroxyphenyl)propan-1-ol is commonly named ifenprodil (**1**, Figure 1). Ifenprodil was initially developed as an α_1 receptor antagonist for the treatment of hypertension.[13] Later, it was found that **1** is a potent negative allosteric modulator selectively inhibiting GluN2B subunit-containing NMDA receptors.[14−16] Commercially available ifenprodil (*unlike* racemate, Cerocral®), which is used in Japan as cerebral vasodilator, showed agonistic activity at σ_1 receptors as well.[17,18] Clinical trials are currently evaluating the therapeutic potential of **1** for the treatment of drug addiction, idiopathic pulmonary fibrosis (IPF), and COVID-19.[19−22] Furthermore, **1** showed positive effects in animal models of Alzheimer's disease and neuropathic pain.[23−25] However, the selectivity of

https://dx.doi.org/10.1021/acs.jmedchem.0c01912
J. Med. Chem. 2021, 64, 1170−1179

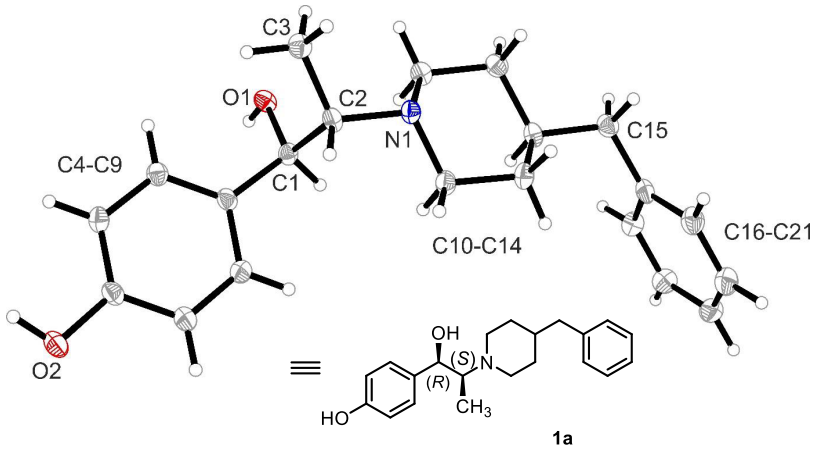

Figure 2. X-ray crystal structure of (1*R*,2*S*)-ifenprodil ((1*R*,2*S*)-**1a**). Thermal ellipsoids are shown at 30% probability. Isomer (1*R*,2*S*)-**1a** crystallized in the chiral space group $P2_12_12_1$. CCDC-2041093.

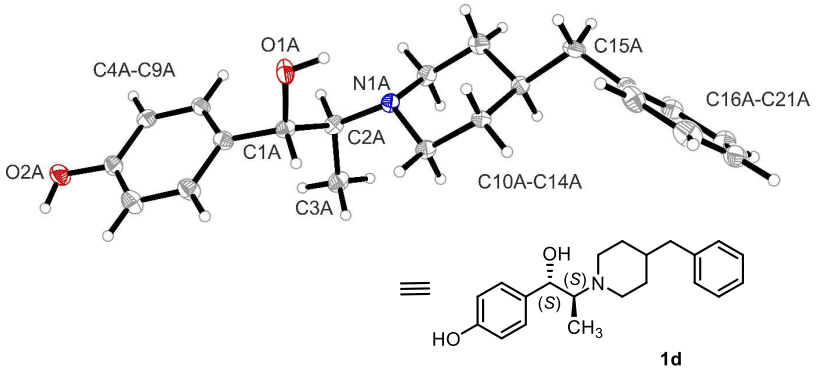

Figure 3. X- ray crystal structure of (1*S*,2*S*)-ifenprodil ((1*S*,2*S*)-**1d**). Thermal ellipsoids are shown at 30% probability. Isomer (1*S*,2*S*)-**1d** crystallized in the chiral space group $P2_1$. CCDC-2041094.

1 over other receptors such as σ_1, σ_2, α_1, 5-HT_{1A}, and 5-HT_2 is rather low[26−29] and depends on the configuration.[27]

The stereodescriptors *erythro* and *threo* are widely used to specify the ifenprodil diastereomers. However, the literature often lacks information about absolute configuration, or given information is misleading; e.g., the stereodescriptor *erythro* is sometimes used for *like*-ifenprodil.[30] The name ifenprodil without specifying stereodescriptor is often used for racemic *threo*-ifenprodil[31−33] but also for the mixture of all four stereoisomers.[34] Biological data are generally correlated with the specific optical rotation of ifenprodil stereoisomers, e.g., (+)-*threo*- or (−)-*threo*-ifenprodil, rather than providing the absolute configuration.[27,32,35]

GluN2B receptor affinity, inhibitory activity, and affinity to NMDA, non-NMDA, and related receptors are only reported for mixtures of diastereomers or without information about the absolute configuration of used ifenprodil stereoisomers. Herein, we wish to report a systematic study on the relative and absolute configuration of ifenprodil stereoisomers and the unequivocal correlation of the different stereoisomers with their pharmacological activity.

2. RESULTS AND DISCUSSION

2.1. Chemistry. As reported in the literature,[27] the synthesis of ifenprodil stereoisomers started with acylation of phenol (**2**) with racemic 2-bromopropionyl bromide in triflic acid. After *Fries* rearrangement of the intermediate ester, 2-bromopropiophenone **3** was isolated in 69% yield. The S_N2 reaction of α-bromoketone **3** with 4-benzylpiperidine afforded racemic α-piperidinylketone **4** in 86% yield. Treatment of ketone **4** with KBH_4 in ethanol led stereoselectively to *unlike*-ifenprodil (**1ab**).[27] Alternatively, ketone **4** was reduced with $LiAlH_4$ in THF according to the procedure of Chenard et al.[27] to provide a mixture of *like*-ifenprodil (**1cd**) and *unlike*-ifenprodil (**1ab**) in the ratio 90:10. (Scheme 1). The relative configuration was determined by ^{1}H NMR spectroscopy and comparison of the spectra with spectra reported in the literature.[27]

The enantiomers of the racemic mixtures **1ab** and **1cd** were separated by preparative chiral HPLC. The *unlike*-enantiomers **1a** and **1b** were separated by Daicel Chiralpak IA using isohexane/iPrOH/MeOH = 93/5/2 with addition of 0.1% Et_2NH as eluent (see Figure S1). For the *like*-enantiomers **1c** and **1d**, the same chiral stationary phase, but isohexane/MeOH = 97/3 + 0.1% Et_2NH as the mobile phase, was used (see Figure S2). All four ifenprodil stereoisomers were isolated with high enantiomeric excess (ee = 99.4−99.8%, see Figures S1 and S2). During the preparative chiral HPLC, a small amount of *N*-oxides of the enantiomerically pure ifenprodil-stereoisomers **1a−d** was formed. Thus, **1a−d** were purified by a second preparative HPLC using a RP-18 stationary phase (see Figures S3 and S4).

Previously, an X-ray crystal structure of racemic *like*-ifenprodil (**1cd**) has been reported.[36] Furthermore, the absolute configuration of (1*S*,2*S*)-configured ifenprodil ((1*S*,2*S*)-**1d**) has been determined by chiral pool synthesis.[37]

https://dx.doi.org/10.1021/acs.jmedchem.0c01912
J. Med. Chem. 2021, 64, 1170−1179

Table 1. Interaction of Ifenprodil Stereoisomers with NMDA Receptors Containing the GluN2B Subunit

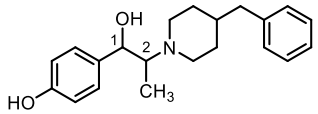

1a-d

	GluN2B affinity	TEVC activity at GluN2B-NMDA			
compd	K_i ± SEM [nM]	IC_{50} ± SE [nM][a]	A_2 ± SE [%][b]	hill slope ± SE	eudismic ratio[c]
(1*R*,2*S*)-**1a**	14.4 ± 3.3	200 ± 28	91 ± 3	1.1 ± 0.2	3.5
(1*S*,2*R*)-**1b**	7.8 ± 0.2	698 ± 46	84 ± 2	1.3 ± 0.1	
(1*R*,2*R*)-**1c**	5.8 ± 1.3[d]	218 ± 16	93 ± 2	1.3 ± 0.1	2.5
(1*S*,2*S*)-**1d**	13.5 ± 2.8	525 ± 32	91 ± 2	1.97 ± 0.18	

[a]Inhibition of (S) glutamate/glycine induced ion flux determined in TEVC experiments. [b]A_2 is the maximum inhibition of ion flux in TEVC experiments at c(**1a–d**) = 30 μM. [c]The eudismic ratio refers to the inhibition of ion flux in TEVC experiments. [d]One-way ANOVA with post hoc Newman Keuls multiple comparison test was used to evaluate the significance of mean differences for GluN2B affinity. The differences of GluN2B affinity for (1*R*,2*R*)-**1c** vs (1*S*,2*S*)-**1d** and (1*R*,2*R*)-**1c** vs (1*R*,2*S*)-**1a** ($p < 0.05$) are significant, and all other differences are not significant.

In order to determine the absolute configuration of all ifenprodil-isomers, an enantiomer of each diastereomer (**1a** and **1d**) was crystallized, and the structures were determined by X-ray crystal structure analysis (Figures 2 and 3).

Two crystallographically independent molecules identified as two conformers (named with suffixes A and B) were found in the asymmetric unit (see Supporting Information). The essential difference between the conformers A and B is the orientation of the phenyl group of the terminal benzyl moiety: in conformer A, a dihedral angle C11−C12−C15−C16 of 68.5(7)° and for conformer B a dihedral angle of 171.3(5) were found. Only conformer A will be further discussed.

The structures of both ifenprodil isomers (1*R*,2*S*)-**1a** and (1*S*,2*S*)-**1d** show a chair conformation for the piperidine ring. Both substituents at the piperidine ring adopt the energetically favored equatorial position, respectively. However, the orientation of the substituents at the ethylene bridge in the structure of both diastereomers differs considerably. Whereas the dihedral angle between the OH and CH_3 moieties (O1−C1−C2−C3) of (1*R*,2*S*)-**1a** is 39.3(4)°, the dihedral angle of the same substituents of the diastereomer (1*S*,2*S*)-**1d** is 176.3(5)°. Moreover, the relative orientation of the hydroxyphenyl ring and the piperidine ring is quite different. Regarding the orientation of these moieties, the dihedral angle (C4−C1−C2−N1) is 146.4(3)° for (1*R*,2*S*)-**1a** and 170.0(5)° for (1*S*,2*S*)-**1d**.

Additionally, CD spectroscopy was used to characterize the four stereoisomers, allowing us to confirm the absolute configuration of (1*S*,2*R*)-**1b** and (1*R*,2*R*)-**1c**, based on their respective Cotton effects (see Figures S9 and S10).

2.2. Pharmacological Evaluation. At first, the relationship between the absolute configuration and the affinity toward the NMDA receptor containing the GluN2B subunit should be investigated by competitive receptor binding assays. In the assay, racemic [^{3}H]-*unlike*-ifenprodil (**1ab**) was used as a radioligand. Membrane fragments of L(tk-)cells stably expressing recombinant human GluN1a and GluN2B subunits of the NMDA receptor were employed as receptor material.[38]

With K_i values between 5.8 nM and 14.4 nM, all four ifenprodil stereoisomers bind with very high affinity to the GluN2B subunit containing NMDA receptors (Table 1). Nevertheless, the ifenprodil isomer (1*R*,2*R*)-**1c** (K_i = 5.8 nM) shows significantly higher GluN2B affinity than its enantiomer (1*S*,2*S*)-**1d** (K_i = 13.5 nM) and its diastereomer (1*R*,2*S*)-**1a** (K_i = 14.4 nM). Thus, (1*R*,2*R*)-**1c** is the eutomer with a eudismic ratio of approximately 2. The GluN2B affinity of the enantiomers (1*R*,2*S*)-**1a** and (1*S*,2*R*)-**1b** does not differ significantly.

Next the inhibition of the (*S*)-glutamate and glycine stimulated ion flux by the ifenprodil stereoisomers was determined by two-electrode voltage clamp (TEVC) measurements on GluN1a/GluN2B expressing *Xenopus laevis* oocytes.[39] Addition of 10 μM (*S*)-glutamate and 10 μM glycine led to ion channel opening. Subsequent application of different concentrations of enantiomerically pure ifenprodil stereoisomers resulted in reduced ion flow. The recorded dose response curves allowed us to evaluate the activity of the test compounds (Table 1 and Figure 4).

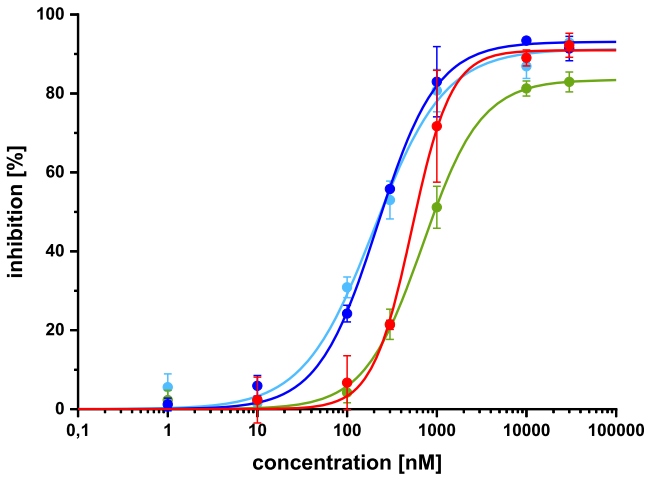

Figure 4. Inhibition curves of (1*R*,2*S*)-**1a** (light blue), (1*S*,2*R*)-**1b** (green), (1*R*,2*R*)-**1c** (dark blue), and (1*S*,2*S*)-**1d** (red). Each data point represents the mean ± SEM of three independent experiments (n = 3).

In TEVC experiments, isomers with (1*R*)-configuration, i.e., (*R*)-configuration at the chiral center with the benzylic OH moiety, showed a stronger inhibitory activity than the stereoisomers with (1*S*)-configuration (Table 1, Figure 4). A similar result was obtained previously for other GluN2B antagonists derived from ifenprodil.[39,40] The increase of activity associated with (1*R*)-configuration is not affected by the configuration of the adjacent center of chirality. A correlation between *like*- and *unlike*-configured ifenprodil

https://dx.doi.org/10.1021/acs.jmedchem.0c01912
J. Med. Chem. 2021, 64, 1170−1179

Table 2. Affinity of Ifenprodil Stereoisomers Toward the GluN2B Subunit Containing NMDA Receptors, α Receptors, and σ Receptors

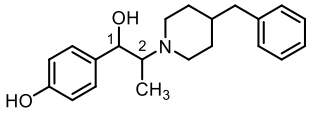

1a-d

	$K_i \pm$ SEM [nM][a]				
compd	GluN2B	α_{1A}	α_{2A}	σ_1	σ_2
(1*R*,2*S*)-**1a**	14.4 ± 3.3	140 ± 27	1600 ± 67	22 ± 3	4.6 ± 2.3
(1*S*,2*R*)-**1b**	7.8 ± 0.16	27 ± 7.2	2300 ± 590	75 ± 29	15 ± 2
(1*R*,2*R*)-**1c**	5.8 ± 1.3	370 ± 150	5500 ± 1600	96 ± 24	6.5 ± 0.8
(1*S*,2*S*)-**1d**	13.5 ± 2.8	530 ± 150	6100 ± 780	278 ± 43	8.6 ± 2.1

[a] K_i values ± SEM values represent the mean of three experiments (n = 3).

stereoisomers and ion channel blocking activity could not be observed. Altogether, the enantiomers (1*R*,2*S*)-**1a** and (1*R*,2*R*)-**1c** represent the eutomers, respectively. However, the eudismic ratios for both pairs of enantiomers are rather low.

Since ifenprodil had originally been developed as an α_1 receptor antagonist for the treatment of hypertension, the affinity toward α_{1A} and α_{2A} receptors was examined in radioligand receptor binding studies. In the α_{1A} and α_{2A} assays, the radioligands [^{3}H]prazosin and [^{3}H]RX821002 were used, respectively.[41,42] Isomer (1*S*,2*R*)-**1b** displays high affinity toward the α_{1A} receptor (K_i = 27 nM). Its enantiomer (1*R*,2*S*)-**1a** has considerably lower α_{1A} affinity resulting in higher selectivity for the GluN2B binding site (Table 2). The α_{1A} receptor affinity of the *like*-configured enantiomers (1*R*,2*R*)-**1c** and (1*S*,2*S*)-**1d** was even lower. Thus, (1*R*,2*R*)-**1c** represents the ifenprodil stereoisomer with the highest selectivity (64-fold) for GluN2B-NMDA receptors over α_{1A} receptors. All four ifenprodil stereoisomers exhibit very high selectivity over the α_{2A} receptor, since the $K_i(\alpha_{2A})$ values are generally higher than 1 μM (Table 2).

As high σ receptor affinity has been reported for ifenprodil, the σ_1 and σ_2 receptor affinities of the ifenprodil stereoisomers were recorded as previously reported.[43−45] In brief, the ifenprodil stereoisomers competed with the radioligands [^{3}H](+)-pentazocine and [^{3}H]di-*o*-tolylguanidine for σ_1 and σ_2 receptors in guinea pig brain and rat liver membrane preparations, respectively. Since [^{3}H]-di-*o*-tolylguanidine also binds to σ_1 receptors, an excess of nonradioactive (+)-pent-azocine was added in the σ_2 assay to mask σ_1 receptors.

Stereoisomer (1*R*,2*S*)-**1a** interacts with high affinity with σ_1 receptors (K_i = 22 nM) and σ_2 receptors (K_i = 4.6 nM). Thus, it can be concluded that the *unlike*-configured ifenprodil stereoisomer (1*R*,2*S*)-**1a** does not bind selectively to GluN2B subunit-containing NMDA receptors (Table 2). Moreover, all ifenprodil isomers bind with high affinity to the σ_2 receptor. However, ifenprodil stereoisomers (1*R*,2*R*)-**1c** and (1*S*,2*S*)-**1d** are selective for the GluN2B binding site over the σ_1 receptor.

It has been previously reported that ifenprodil binds to the 5-HT$_{1A}$ and 5-HT$_2$ receptors.[27] Drugs acting as 5-HT$_{1A}$ receptor agonist (e.g., buspirone) or 5-HT$_{2B}$ receptor antagonist (e.g., SB204741) have shown antihypertensive effects.[46] Moreover, several 5-HT receptor subtypes influence NMDA receptor signaling.[47−51] (1*S*,2*R*)-**1b** shows high affinity for the 5-HT$_{1A}$ and the 5-HT$_{2B}$ receptor, whereas its enantiomer (1*R*,2*S*)-**1a** only exhibits high-affinity binding for the 5-HT$_{2B}$ receptor. (1*R*,2*R*)-**1c** and (1*S*,2*S*)-**1d** bind with moderate affinity to the 5-HT$_{2A}$ receptor (K_i = 338 nM and 369 nM, respectively) but can be considered to be selective for the GluN2B receptor over all tested serotonin receptor subtypes.

Table 3. Affinity of Ifenprodil Stereoisomers Toward Different Types of 5-HT Receptors

	K_i [nM][a]					
compd	5-HT$_{1A}$	5-HT$_{2A}$	5-HT$_{2B}$	5-HT$_{2C}$	5-HT$_6$	5-HT$_7$
(1*R*,2*S*)-**1a**	>1000	421	95	748	>1000	513
(1*S*,2*R*)-**1b**	46	510	66	>10000	>1000	>10000
(1*R*,2*R*)-**1c**	>1000	338	708	>10000	>10000	>10000
(1*S*,2*S*)-**1d**	>1000	369	>1000	>10000	>10000	>10000

[a] K_i values represent the mean of two experiments (n = 2 with duplicate points).

3. CONCLUSION

After determination of the absolute configuration by X-ray structure analysis and CD spectroscopy, the GluN2B affinity, selectivity, and inhibitory activity of all enantiomerically pure ifenprodil stereoisomers were evaluated. In receptor binding studies using [^{3}H]ifenprodil as a competing radioligand, the GluN2B affinity of the four stereoisomers is very similar (K_i = 5.8−14.4 nM). It can be concluded that the configuration of the two centers of chirality does not influence considerably the binding to the ifenprodil binding site of GluN2B subunit containing NMDA receptors. However, NMDA receptor inhibitors have been shown to not always present a strict affinity−activity relationship.[38]

Stereoisomers with (1*R*)-configuration of the center of chirality in benzylic position showed higher inhibitory activity in TEVC experiments than the corresponding (1*S*)-configured stereoisomers. Thus, it can be concluded that (*R*)-configuration at the benzylic center of chirality is important for elevated inhibitory activity. On the contrary, the configuration at the 2-position is less important for ion channel inhibition.

The ifenprodil stereoisomers only weakly interact with α_{2A} receptors. A considerable α_{1A} receptor affinity was found only for (1*S*,2*R*)-**1b** displaying a K_i value of 27 nM. However, this stereoisomer inhibited only weakly the NMDA receptor associated ion channel (IC_{50} = 698 nM) indicating a preference for the α_{1A} receptor over the GluN2B receptor. On the

https://dx.doi.org/10.1021/acs.jmedchem.0c01912
J. Med. Chem. 2021, 64, 1170−1179

contrary, the most active GluN2B antagonist (1*R*,2*R*)-**1c** shows high selectivity over α_{1A} (64-fold) and α_2 receptors (~1000-fold). Thus, the GluN2B inhibitory activity and the α_1 receptor affinity can be separated by variation of the stereochemistry, an effect to be considered for the clinical development of ifenprodil.

With exception of (1*R*,2*S*)-**1a**, the ifenprodil stereoisomers exhibit 10−20-fold selectivity for GluN2B receptors over σ_1 receptors. However, all stereoisomers possess low nanomolar σ_2 affinity. It can be concluded that the GluN2B:σ_1 receptor selectivity can be controlled by the stereochemistry, but the affinity toward σ_2 receptors cannot be eliminated or reduced by changing the configuration. This interesting finding indicates that a NMDA receptor inhibitor with high σ_1 affinity is available. Thus, (1*R*,2*S*)-**1a** might have a pharmacological profile beneficial in the context of an antiflashback therapy of post-traumatic stress disorder (PTSD).[17,52] On the other hand, a higher NMDA receptor selectivity without reduced σ_1 receptor affinity may be beneficial in the context of an antiapoptotic therapy counteracting excitotoxicity in stroke, Parkinson's disease, Alzheimer's disease, and Huntington's disease.[3−5]

During testing of serotonin receptor affinity (5-HT_{1A}, 5-HT_{2A}, 5-HT_{2B}, 5-HT_{2C}, 5-HT_6, 5-HT_7) moderate 5-HT_{1A} and 5-HT_{2B} affinity was detected only for both *unlike*-configured enantiomers (1*R*,2*S*)-**1a** and (1*S*,2*R*)-**1b**. The *like*-configured stereoisomers (1*R*,2*R*)-**1c** and (1*S*,2*S*)-**1d** showed only negligible affinity toward the tested serotonin receptors. It can be concluded that the 5-HT-affinity of the ifenprodil stereoisomers is rather low, but appropriate configuration can further increase the selectivity for the GluN2B receptor over the 5-HT receptors.

Altogether, with respect to GluN2B affinity and inhibitory activity, (1*R*,2*R*)-**1c** appears to be the most promising ifenprodil stereoisomer. In addition to high GluN2B affinity and inhibitory activity, (1*R*,2*R*)-**1c** shows high selectivity over α_{1A}, α_{2A}, σ_1, and six 5-HT receptors. Only the cross reactivity at σ_2 receptors could not be eliminated or reduced by changing the stereochemistry. Thus, (1*R*,2*R*)-**1c** selectively targeting GluN2B subunit-containing NMDA receptors could be beneficial in antiapoptotic therapy resulting in fewer side effects. Additionally, the NMDA receptor inhibitor (1*R*,2*S*)-**1a** with high σ_1 affinity could be beneficial in the treatment of PTSD.

In summary, we systematically correlated the absolute configuration of all four ifenprodil stereoisomers with their pharmacological properties. Two ifenprodil stereoisomers with unique pharmacological profiles were identified, which may be beneficial in different specific clinical contexts.

4. EXPERIMENTAL SECTION

4.1. Chemistry. *4.1.1. General Methods.* Thin layer chromatography (tlc): tlc silica gel 60 F_{254} on aluminum sheets (VWR). MS: MicroTOFQII mass spectrometer (Bruker Daltonics, Bremen, Germany); deviations of the found exact masses from the calculated exact masses were 5 ppm or less; the data were analyzed with DataAnalysis (Bruker Daltonics). NMR: NMR spectra were recorded in deuterated solvents on Agilent DD2 400 and 600 MHz spectrometers (Agilent, Santa Clara CA, USA); chemical shifts (δ) are reported in parts per million (ppm) against the reference substance tetramethylsilane and calculated using the solvent residual peak of the undeuterated solvent; coupling constants are given with 0.5 Hz resolution; assignment of ^{1}H and ^{13}C NMR signals was supported by 2-D NMR techniques where necessary.

4.1.2. HPLC Method 1 for the Determination of the Purity. Equipment 1: Pump: L-7100, degasser: L-7614, autosampler: L-7200, UV detector: L-7400, interface: D-7000, data transfer: D-line, data acquisition: HSM-Software (all from Merck Hitachi, Darmstadt, Germany); Equipment 2: Pump: LPG-3400SD, degasser: DG-1210, autosampler: ACC-3000T, UV-detector: VWD-3400RS, interface: DIONEX UltiMate 3000, data acquisition: Chromeleon 7 (equipment and software from Thermo Fisher Scientific, Lauenstadt, Germany); column: LiChrospher 60 RP-select B (5 μm), LiChroCART 250−4 mm cartridge; flow rate: 1.0 mL/min; injection volume: 5.0 μL; detection at λ = 210 nm; solvents: A: demineralized water with 0.05% (V/V) trifluoroacetic acid, B: CH_3CN with 0.05% (V/V) trifluoroacetic acid; gradient elution (% A): 0−4 min: 90%; 4−29 min: gradient from 90% to 0%; 29−31 min: 0%; 31−31.5 min: gradient from 0% to 90%; 31.5−40 min: 90%. Unless otherwise mentioned, the purity of all test compounds is greater than 95%.

*4.1.3. Preparative HPLC Method 2A for Separation of the Enantiomers (1R,2S)-**1a** and (1S,2R)-**1b**.* Merck Hitachi equipment; UV detector: L-7400; interface D-7000, autosampler: L-7200; pump: L-7150A; data acquisition: HSM-software; guard column: Daicel Chiralpak IA; column: 5 μm, 10 mm/20 mm, Daicel Chiralpak IA, 5 μm, 250 mm/20 mm; flow rate: 0−0.5 min 5 mL/min, 0.5−130 min 15 mL/min; injection: volume: 400 μL (isohexane/iPrOH); detection λ = 275 nm; eluent: isohexane/iPrOH/MeOH = 93/5/2 + 0.1% Et_2NH.

*4.1.4. Preparative HPLC Method 2B for Separation of the Enantiomers of (1R,2R)-**1c** and (1S,2S)-**1d**.* Merck Hitachi equipment; UV detector: L-7400; interface D-7000, autosampler: L-7200; pump: L-7150A; data acquisition: HSM-software; guard column: Daicel Chiralpak IA; column: 5 μm, 10 mm/20 mm, Daicel Chiralpak IA, 5 μm, 250 mm/20 mm; flow rate: 0−0.5 min 5 mL/min, 0.5−130 min 15 mL/min; injection: volume: 400 μL (isohexane/MeOH); detection λ = 275 nm; eluent: isohexane/MeOH = 97/3 + 0.1% Et_2NH.

*4.1.5. Chiral HPLC Method 3A to Determine the Enantiomeric Purity of (1R,2S)-**1a** and (1S,2R)-**1b**.* Merck Hitachi equipment; DAD detector: L-7455; interface D-7000, Rheodyne 7725i; pump: L-6200A; data acquisition: HSM-software; Daicel Chiralpak IA, 5 μm, 10 mm/4 mm; column: Daicel Chiralpak IA, 5 μm, 250 mm/4.6 mm; flow rate: 1.00 mL/min; injection: volume: 5.0 μL; detection λ = 275 nm; eluent: isohexane/iPrOH/MeOH = 93/5/2 + 0.1% Et_2NH.

*4.1.6. Chiral HPLC Method 3B to Determine the Enantiomeric Purity of (1R,2R)-**1c** and (1S,2S)-**1d**.* Merck Hitachi equipment; DAD detector: L-7455; interface D-7000, Rheodyne 7725i; pump: L-6200A; data acquisition: HSM-software; Daicel Chiralpak IA, 5 μm, 10 mm/4 mm; column: Daicel Chiralpak IA, 5 μm, 250 mm/4.6 mm; flow rate: 1.00 mL/min; injection: volume: 5.0 μL; detection λ = 275 nm; eluent: isohexane/MeOH = 97/3 + 0.1% Et_2NH.

*4.1.7. Preparative HPLC Method 4A for Separation of the Enantiomers (1R,2S)-**1a** and (1S,2R)-**1b** from Their N-Oxides.* Merck Hitachi equipment; UV detector: L-7400; interface D-7000; autosampler: L-7200; pump: L-7100; degasser: L-7614; column: Phenomenex Gemini C18 110 Å, 250−21.2 mm; 15−21.2 mm security guard; flow rate: 9 mL/min; injection: volume: 100 μL; detection λ = 210 nm; eluent: acetonitrile/H_2O 7/3 + 0.1% ammonia.

*4.1.8. Preparative HPLC Method 4B for Separation of the Enantiomers of (1R,2R)-**1c** and (1S,2S)-**1d** from Their N-Oxides.* Merck Hitachi equipment; UV detector: L-7400; interface D-7000; autosampler: L-7200; pump: L-7100; degasser: L-7614; column: Phenomenex Gemini C18 110 Å, 250−21.2 mm; 15−21.2 mm security guard; flow rate: 9 mL/min; injection: volume: 100 μL; detection λ = 210 nm; eluent: acetonitrile/H_2O 9/1 + 0.1% ammonia.

*4.1.9. (1R,2S)- and (1S,2R)-2-(4-benzylpiperidin-1-yl)-1-(4-hydroxyphenyl)propan-1-ol ((1R,2S)-**1a** and (1S,2R)-**1b**): Separation by Chiral HPLC.* The two enantiomers were separated by chiral preparative HPLC (HPLC method 2A). (1*S*,2*R*)-**1b**: t_R = 20.8 min; (1*R*,2*S*)-**1a**: t_R = 24.2 min. The solvent was removed in vacuo, respectively. The single enantiomers were separated from their N-oxides by preparative HPLC method 4A. *N*-Oxide: t_R = 3.1 min, (1*R*,2*S*)-**1a**/(1*S*,2*R*)-**1b**: t_R = 7.7 min. The solvent was removed in vacuo, respectively.

https://dx.doi.org/10.1021/acs.jmedchem.0c01912
J. Med. Chem. 2021, 64, 1170−1179

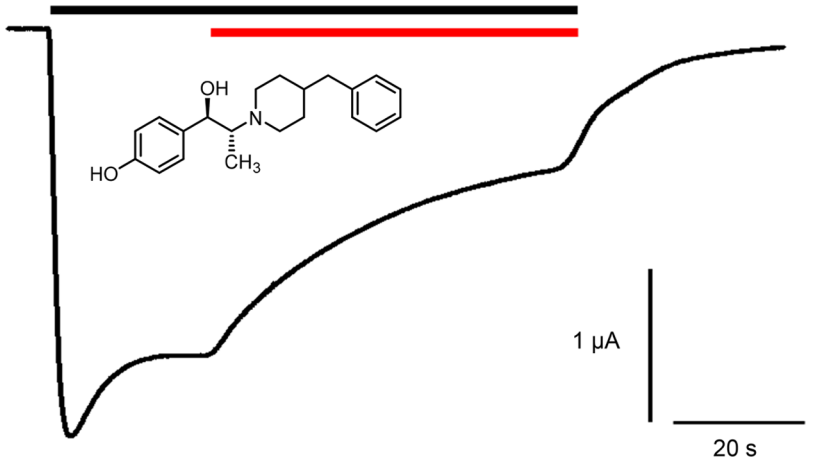

Figure 5. Representative current trace of GluN1−1a/GluN2B expressing oocytes activated with 10 μM (*S*)-glutamate and 10 μM glycine (black bar) and treated subsequently with (1*R*,2*R*)-**1c** (red bar). Current traces of all stereoisomers **1a**−**d** (c = 300 nM) are shown in the Supporting Information (see Figure S3).

(1*R*,2*S*)-**1a**: HPLC (method 1): t_R = 16.4 min, purity 99.2%. HPLC (method 3A): t_R = 24.2 min, ratio of enantiomers 99.8:0.2 (99.6% ee).

(1*S*,2*R*)-**1b**: HPLC (method 1): t_R = 16.5 min, purity 98.0%. HPLC (method 3A): t_R = 20.8 min, ratio of enantiomers 99.6:0.4 (99.2% ee).

*4.1.10. (1R,2R)- and (1S,2S)-2-(4-benzylpiperidin-1-yl)-1-(4-hydroxyphenyl)propan-1-ol ((1R,2R)-**1c** and (1S,2S)-**1d**): Separation by Chiral HPLC.* The two enantiomers were separated by chiral preparative HPLC (HPLC method 2B) (1*R*,2*R*)-**1c**: t_R = 39.0 min; (1*S*,2*S*)-**1d**: t_R = 42.9 min). The solvent was removed in vacuo, respectively. The single enantiomers were separated from their N-oxides by preparative HPLC method 4B. *N*-oxide: t_R = 3.0 min; (1*R*,2*R*)-**1c**/(1*S*,2*S*)-**1d**: t_R = 11.8 min. The solvent was removed in vacuo, respectively.

(1*R*,2*R*)-**1c**: HPLC (method 1): t_R = 16.6 min, purity 97.6%. HPLC (method 3B): t_R = 39.0 min, ratio of enantiomers 99.4:0.6 (98.8% ee).

(1*S*,2*S*)-**1d**: HPLC (method 1): t_R = 16.5 min, purity 98.3%. HPLC (method 3B): t_R = 42.9 min, ratio of enantiomers 99.5:0.5 (99.0% ee).

4.1.11. Synthetic Procedures. Synthetic procedures and parts of the spectroscopic data have been previously reported by Chenard et al.[27] and can be found in the Supporting Information.

4.2. X-ray Crystallography. CCDC-2041093 for (1*R*,2*S*)-**1a** and -2041094 for (1*S*,2*S*)-**1d** contain the supplementary crystallographic data for this paper. These data can be obtained free of charge from The Cambridge Crystallographic Data Centre via www.ccdc.cam.ac.uk/data_request/cif.

4.3. Pharmacological Evaluation. *4.3.1. Radioligand Receptor Binding Studies.* The affinity toward the ifenprodil binding site of GluN2B subunit containing NMDA receptors was recorded as described in refs 38 and 53. Performance of the σ_1 and σ_2 assays is reported in refs 43−45. The corresponding procedures are given in the Supporting Information.

4.3.2. GluN2B Binding Assay. The competitive binding assay was performed with the radioligand [^{3}H]ifenprodil (60 Ci/mmol; BIOTREND, Cologne, Germany). The thawed cell membrane preparation from the transfected L(tk-) cells (about 20 μg of protein) was incubated with various concentrations of test compounds, 5 nM [^{3}H]ifenprodil, and TRIS/EDTA-buffer (5 mM TRIS/1 mM EDTA, pH 7.5) at 37 °C. The nonspecific binding was determined with 10 μM unlabeled ifenprodil. The K_d value of ifenprodil is 7.6 nM.[38]

4.3.3. Molecular Biology and TEVC Experiments. Molecular biology and TEVC experiments were conducted as described before by Schreiber et al.[39,40] In brief, stage V defoliated *Xenopus laevis* oocytes were obtained from EcoCyte Bioscience (Dortmund, Germany), and oocytes were injected with 0.8 ng of cRNA of each subunit (GluN1a/GluN2B) *in vitro* transcribed from linearized cDNA templates with Ambion T7 mMessage mMachine kit (Life Technologies, Darmstadt, Germany) using nanoliter injector 2000 (WPI, Berlin, Germany). Injected oocytes were stored for 5−6 days at 16 °C in Bath's solution containing (mmol/L): 88 NaCl, 1 KCl, 0.4 $CaCl_2$, 0.33 $Ca(NO_3)_2$, 0.6 $MgSO_4$, 5 Tris-HCl, 2.4 $NaHCO_3$ and supplemented with 80 mg/L theophylline, 63 mg/L penicillin, 40 mg/L streptomycin, and 100 mg/L gentamycin.

TEVC recordings were conducted at room temperature using a Turbo Tec 10CX amplifier (NPI electronic, Tamm, Germany), NI USB 6221 DA/AD Interface (National Instruments, Austin, USA) and *GePulse* Software (Dr. Michael Pusch, Genova, Italy). The oocytes were perfused with Ba^{2+}-Ringer solution containing (mmol/L): 10 HEPES, 90 NaCl, 1 KCl, 1.5 $BaCl_2$ (pH was adjusted to 7.4 with 1 M NaOH) during measurements. The agonist solution contained 10 μM each of glycine and (*S*)-glutamate, which was added from 100 mM stock solutions of glycine and (*S*)-glutamate prior experimentation. The test compound solutions were freshly prepared from 10 mM DMSO stock solutions. The holding potential was set to −70 mV, and recording pipettes backfilled with 3 M KCl had resistances in the range of 0.5−1.5 MΩ.

4.3.4. Data Analysis and Statistics. The data were analyzed using custom software Ana (Dr. Michael Pusch, Genova, Italy) and OriginPro 2020. Inhibition was calculated by the following equation:

$$\text{inhibition} = 1 - \frac{Ic - Ib}{Ia - Ib}$$

where Ic is the current in the presence of the compound solution, Ib is the holding current before adding agonist solution and Ia is the current after adding agonist solution.

Data Analysis was done using Origin Pro 2020 (OriginLab Corporation, Northampton, MA, USA). Dose−response curves were fitted to the logistic sigmoid equation:

$$y = \frac{\text{A1} - \text{A2}}{1 + \left(\frac{x}{x_0}\right)^p} + A2$$

A1 and A2 represent the minimal and maximal inhibition of ion flux by a compound. A1 was determined as A1 = 0%, whereas A2 was kept flexible. x_0 is the concentration at half-maximum inhibition, and x is the examined concentration. p is the slope of the curve.

■ ASSOCIATED CONTENT

Supporting Information

The Supporting Information is available free of charge at https://pubs.acs.org/doi/10.1021/acs.jmedchem.0c01912.

https://dx.doi.org/10.1021/acs.jmedchem.0c01912
J. Med. Chem. 2021, 64, 1170−1179

Purity data of all test compounds, synthesis of the ketones **3** and **4**, chiral HPLC chromatograms of all four enantiomerically pure ifenprodil stereoisomers, enantiomeric purity data, experimental procedures of receptor binding studies, X-ray crystallographic data of **1a** and **1d**, ^{1}H and ^{13}C NMR spectra, CD spectra and HPLC chromatograms of all four ifenprodil stereoisomers (PDF)

Molecular formula strings (CSV)

Accession Codes

Authors will release the atomic coordinates and experimental data upon article publication. PDB IDs have been provided in Figures 2 and 3, in section 4.2. X-ray crystallography and in the Supporting Information. (1*R*,2*S*)-**1a**: CCDC-2041093; (1*S*,2*S*)-**1d**: CCDC-2041094.

AUTHOR INFORMATION

Corresponding Author

Bernhard Wünsch − *GRK 2515, Chemical Biology of Ion Channels (Chembion) and Institut für Pharmazeutische und Medizinische Chemie, Westfälische Wilhelms-Universität Münster, D-48149 Münster, Germany;* orcid.org/0000-0002-9030-8417; Phone: +49-251-8333311; Email: wuensch@uni-muenster.de; Fax: +49-8332144

Authors

Elena Bechthold − *GRK 2515, Chemical Biology of Ion Channels (Chembion) and Institut für Pharmazeutische und Medizinische Chemie, Westfälische Wilhelms-Universität Münster, D-48149 Münster, Germany*

Julian A. Schreiber − *Institut für Pharmazeutische und Medizinische Chemie, Westfälische Wilhelms-Universität Münster, D-48149 Münster, Germany; Cellular Electrophysiology and Molecular Biology, Institute for Genetics of Heart Diseases (IfGH), Department of Cardiovascular Medicine, University Hospital Münster, D-48149 Münster, Germany*

Kirstin Lehmkuhl − *Institut für Pharmazeutische und Medizinische Chemie, Westfälische Wilhelms-Universität Münster, D-48149 Münster, Germany*

Bastian Frehland − *Institut für Pharmazeutische und Medizinische Chemie, Westfälische Wilhelms-Universität Münster, D-48149 Münster, Germany*

Dirk Schepmann − *Institut für Pharmazeutische und Medizinische Chemie, Westfälische Wilhelms-Universität Münster, D-48149 Münster, Germany*

Freddy A. Bernal − *Institut für Pharmazeutische Biologie und Phytochemie, Westfälische Wilhelms-Universität Münster, D-48149 Münster, Germany*

Constantin Daniliuc − *Organisch-chemisches Institut, Westfälische Wilhelms-Universität Münster, D-48149 Münster, Germany;* orcid.org/0000-0002-6709-3673

Inés Álvarez − *In Vitro Pharmacology, WeLab, Parc Cientific de Barcelona, 08028 Barcelona, Spain*

Cristina Val Garcia − *Grupo de Investigación Biofarma. Departamento de Farmacología, Farmacia y Tecnología Farmacéutica. Centro de Investigación CIMUS, Universidad de Santiago de Compostela, 15782 Santiago de Compostella, Spain*

Thomas J. Schmidt − *Institut für Pharmazeutische Biologie und Phytochemie, Westfälische Wilhelms-Universität Münster, D-48149 Münster, Germany;* orcid.org/0000-0003-2634-9705

Guiscard Seebohm − *GRK 2515, Chemical Biology of Ion Channels (Chembion), Westfälische Wilhelms-Universität Münster, D-48149 Münster, Germany; Cellular Electrophysiology and Molecular Biology, Institute for Genetics of Heart Diseases (IfGH), Department of Cardiovascular Medicine, University Hospital Münster, D-48149 Münster, Germany; Grupo de Investigación Biofarma. Departamento de Farmacología, Farmacia y Tecnología Farmacéutica. Centro de Investigación CIMUS, Universidad de Santiago de Compostela, 15782 Santiago de Compostella, Spain*

Complete contact information is available at: https://pubs.acs.org/10.1021/acs.jmedchem.0c01912

Notes

The authors declare no competing financial interest.

ACKNOWLEDGMENTS

This work was supported by the Research Training Group "Chemical biology of ion channels (Chembion)" funded by the Deutsche Forschungsgemeinschaft (DFG), which is gratefully acknowledged. We thank Prof. Dr. Peter Gmeiner and Dr. Harald Hübner, Friedrich-Alexander-Universität Erlangen, for recording the α receptor affinity. Furthermore, we thank Dr. Jens Köhler for his help with NMR spectroscopy and Luca Blicker and Marvin Korff for critical proofreading.

ABBREVIATIONS USED

CD, circular dichroism; 5-HT, 5-hydroxytryptamine (= serotonin); IPF, idiopathic pulmonary fibrosis; *l*, *like*; LTP, long-term potentiation; NMDA, *N*-methyl-D-aspartate; PTSD, post-traumatic stress disorder; TEVC, two electrode voltage clamp; *u*, *unlike*

REFERENCES

(1) Artola, A.; Singer, W. Long-term potentiation and NMDA receptors in rat visual cortex. *Nature* **1987**, *330* (6149), 649−652.

(2) Karakas, E.; Furukawa, H. Crystal structure of a heterotetrameric NMDA receptor ion channel. *Science* **2014**, *344* (6187), 992−997.

(3) Ulas, J.; Weihmuller, F.; Brunner, L. C.; Joyce, J. N.; Marshall, J. F.; Cotman, K. W. Selective increase of NMDA-sensitive glutamate binding in the striatum of Parkinson's disease, Alzheimer's disease, and mixed Parkinson's disease/Alzheimer ' s disease patients: an autoradiographic study. *J. Neurosci.* **1994**, *14* (11), 6317−6324.

(4) Choi, D. W. Ionic dependence of glutamate neurotoxicity. *J. Neurosci.* **1987**, *7* (2), 369−379.

(5) Kelly, B. L.; Ferreira, A. SS-amyloid-induced dynamin 1 degradation is mediated by N -methyl- D -aspartate receptors in hippocampal neurons * □. *J. Biol. Chem.* **2006**, *281* (38), 28079−28089.

(6) Anantharam, V.; Panchal, R. G.; Wilson, A.; Kolchine, V. V.; Treistman, S. N.; Bayley, H. Combinatorial RNA splicing alters the surface charge on the NMDA receptor. *FEBS Lett.* **1992**, *305* (1), 27−30.

(7) Hollmann, M.; Boulter, J.; Maron, C.; Beasley, L.; Sullivan, J.; Pecht, G.; Heinemann, S. Zinc Potentiates Agonist-Induced Currents at Certain Splice Variants of the NMDA Receptor. *Neuron* **1993**, *10* (5), 943−954.

(8) Dingledine, R.; Borges, K.; Bowie, D.; Traynelis, S. F. The Glutamate Receptor Ion Channels. *Pharmacol. Rev.* **1999**, *51* (1), 7−61.

(9) Eriksson, M.; Nilsson, A.; Froelich-Fabre, S.; Åkesson, E.; Dunker, J.; Seiger, Å.; Folkesson, R.; Benedikz, E.; Sundström, E.

Cloning and Expression of the Human N-Methyl-D-Aspartate Receptor Subunit NR3A. *Neurosci. Lett.* **2002**, *321* (3), 177−181.
(10) Wyllie, D. J. A.; Livesey, M. R.; Hardingham, G. E. Influence of GluN2 Subunit Identity on NMDA Receptor Function. *Neuropharmacology* **2013**, *74*, 4−17.
(11) Lipton, S. A. Failures and Successes of NMDA Receptor Antagonists: Molecular Basis for the Use of Open-Channel Blockers like Memantine in the Treatment of Acute and Chronic Neurologic Insults. *NeuroRx* **2004**, *1* (1), 101−110.
(12) Moss, G. P. Basic Terminology of Stereochemistry. *Pure Appl. Chem.* **1996**, *68* (12), 2193−2222.
(13) Carron, C.; Jullien, A.; Bucher, B. Synthesis and Pharmacological Properties of a Series of 2-Piperidino Alkanol Derivatives. *Arzneimittelforschung* **1971**, *12*, 1992−1998.
(14) Williams, K. Ifenprodil Discriminates Subtypes of the N-Methyl-D-Aspartate Receptor: Selectivity and Mechanisms at Recombinant Heteromeric Receptors. *Mol. Pharmacol.* **1993**, *44*, 851−859.
(15) Karakas, E.; Simorowski, N.; Furukawa, H. Subunit Arrangement and Phenylethanolamine Binding in GluN1/GluN2B NMDA Receptors. *Nature* **2011**, *475*, 249−253.
(16) Zarnowski, T.; Kleinrok, Z.; Turski, W. A.; Czuczwar, S. The NMDA antagonist procyclidine, but not ifenprodil, enhances the protective efficacy of common antiepileptics against maximal electroshock-induced seizures in mice. *J. Neural Transm.* **1994**, *97*, 1−12.
(17) Ishima, T.; Hashimoto, K. Potentiation of nerve growth factor-induced neurite outgrowth in PC12 cells by ifenprodil: the role of sigma-1 and IP3 receptors. *PLoS One* **2012**, *7* (5), e37989.
(18) Hashimoto, K. Activation of Sigma-1 Receptor Chaperone in the Treatment of Neuropsychiatric Diseases and Its Clinical Implication. *J. Pharmacol. Sci.* **2015**, *127* (1), 6−9.
(19) Sugaya, N.; Ogai, Y.; Aikawa, Y.; Yumoto, Y.; Takahama, M.; Tanaka, M.; Haraguchi, A.; Umeno, M.; Ikeda, K. A Randomized Controlled Study of the Effect of Ifenprodil on Alcohol Use in Patients with Alcohol Dependence. *Neuropsychopharmacol. Reports* **2018**, *38* (1), 9−17.
(20) Kotajima-Murakami, H.; Takano, A.; Ogai, Y.; Tsukamoto, S.; Murakami, M.; Funada, D.; Tanibuchi, Y.; Tachimori, H.; Maruo, K.; Sasaki, T.; Matsumoto, T.; Ikeda, K. Study of Effects of Ifenprodil in Patients with Methamphetamine Dependence: Protocol for an Exploratory, Randomized, Double-Blind, Placebo-Controlled Trial. *Neuropsychopharmacol. Reports* **2019**, *39* (2), 90−99.
(21) NP-120. https://algernonpharmaceuticals.com/ipf-np-120/.
(22) Algernon Pharmaceuticals Announces 154 Patients Enrolled in its Multinational Phase 2b/3 Human Study of Ifenprodil for COVID-19. https://www.globenewswire.com/news-release/2020/11/23/2131702/0/en/Algernon-Pharmaceuticals-Announces-154-Patients-Enrolled-in-its-Multinational-Phase-2b-3-Human-Study-of-Ifenprodil-for-COVID-19.html.
(23) Huang, Y.; Shen, W.; Su, J.; Cheng, B.; Li, D.; Liu, G.; Zhou, W. X.; Zhang, Y. X. Modulating the Balance of Synaptic and Extrasynaptic NMDA Receptors Shows Positive Effects against Amyloid-β-Induced Neurotoxicity. *J. Alzheimer's Dis.* **2017**, *57* (3), 885−897.
(24) Kim, Y.; Cho, H.; Ahn, Y. J.; Kim, J.; Yoon, Y. W. Effect of NMDA NR2B Antagonist on Neuropathic Pain in Two Spinal Cord Injury Models. *Pain* **2012**, *153* (5), 1022−1029.
(25) Ismail, C. A. N.; Suppian, R.; Abd Aziz, C. B.; Haris, K.; Long, I. Increased Nociceptive Responses in Streptozotocin-Induced Diabetic Rats and the Related Expression of Spinal NR2B Subunit of N-Methyl-D-Aspartate Receptors. *Diabetes Metab. J.* **2019**, *43* (2), 222−235.
(26) Karbon, E. W.; Patch, R. J.; Pontecorvo, M. J.; Ferkany, J. W. Ifenprodil Potently Interacts with [3HI (+) −3-PPP-Labeled o Binding Sites in Guinea Pig Brain Membranes. *Eur. J. Pharmacol.* **1990**, *176*, 247−248.
(27) Chenard, B. L.; Shalaby, I. A.; Koe, B. K.; Ronau, R. T.; Butler, T. W.; Prochniak, M. A.; Schmidt, A. W.; Fox, C. B. Separation of A 1Adrenergic and N-Methyl-D-Aspartate Antagonist Activity in a Series of Ifenprodil Compounds. *J. Med. Chem.* **1991**, *34* (10), 3085−3090.
(28) Mott, D. D.; Doherty, J. J.; Zhang, S.; Washburn, M. S.; Fendley, M. J.; Lyuboslavsky, P.; Traynelis, S. F.; Dingledine, R. Phenylethanolamines Inhibit NMDA Receptors by Enhancing Proton Inhibition. *Nat. Neurosci.* **1998**, *1* (8), 659−667.
(29) McCool, B. A.; Lovinger, D. M. Ifenprodil Inhibition of the 5-Hydroxytryptamine3 Receptor. *Neuropharmacology* **1995**, *34* (6), 621−629.
(30) Chenard, B. L.; Menniti, F. S. Antagonists Selective for NMDA Receptors Containing the NR2B Subunit. *Curr. Pharm. Des.* **1999**, *5*, 381−404.
(31) Liu, W.; Jiang, X.; Zu, Y.; Yang, Y.; Liu, Y.; Sun, X.; Xu, Z.; Ding, H.; Zhao, Q. European Journal of Medicinal Chemistry Review Article A Comprehensive Description of GluN2B-Selective N-Methyl-D- Aspartate (NMDA) Receptor Antagonists. *Eur. J. Med. Chem.* **2020**, *200*, 112447.
(32) Hashimoto, K.; London, E. D. Interactions of Erythro-Ifenprodil, Threo-Ifenprodil, Erythro-Iodoifenprodil, and Eliprodil with Subtypes of σ Receptors. *Eur. J. Pharmacol.* **1995**, *273* (3), 307−310.
(33) Quan, J.; Ma, C.; Wang, Y.; Hu, B.; Zhang, D.; Zhang, Z.; Wang, J.; Cheng, M. Repurposing of Cefpodoxime Proxetil as Potent Neuroprotective Agent through Computational Prediction and in Vitro Validation. *J. Biomol. Struct. Dyn.* **2020**, *0* (0), 1−11.
(34) Borza, I.; Domány, G. NR2B Selective NMDA Antagonists: The Evolution of the Ifenprodil-Type Pharmacophore. *Curr. Top. Med. Chem.* **2006**, *6*, 687−695.
(35) Avenet, P.; Léonardon, J.; Besnard, F.; Graham, D.; Frost, J.; Depoortere, H.; Langer, S. Z.; Scatton, B. Antagonist Properties of the Stereoisomers of Ifenprodil at N R 1 A/N R 2 A and N R 1 A/N R 2 B Subtypes of the NMDA Receptor Expressed in Xenopus Oocytes. *Eur. J. Pharmacol.* **1996**, *296*, 209−213.
(36) Kubicki, M.; Codding, P. W. The Crystal and Molecular Structures of Rac-Threo-Ifenprodil and Two Other 4-Benzylpiperidinyl Derivatives. *J. Chem. Crystallogr.* **2003**, *33* (7), 563−568.
(37) Mantegani, S.; Arlandini, E.; Brambilla, E.; Cremonesi, P.; Varasi, M. An Easy Entry to (1S, 2S) and (1R, 2R)-Threo-Ifenprodil. *Synth. Commun.* **2000**, *30* (19), 3543−3553.
(38) Schepmann, D.; Frehland, B.; Lehmkuhl, K.; Tewes, B.; Wünsch, B. Development of a Selective Competitive Receptor Binding Assay for the Determination of the Affinity to NR2B Containing NMDA Receptors. *J. Pharm. Biomed. Anal.* **2010**, *53* (3), 603−608.
(39) Schreiber, J. A.; Schepmann, D.; Frehland, B.; Thum, S.; Datunashvili, M.; Budde, T.; Hollmann, M.; Strutz-Seebohm, N.; Wünsch, B.; Seebohm, G. A Common Mechanism Allows Selective Targeting of GluN2B Subunit-Containing N-Methyl-D-Aspartate Receptors. *Commun. Biol.* **2019**, *2* (1), 1−14.
(40) Börgel, F.; Szermerski, M.; Schreiber, J. A.; Temme, L.; Strutz-Seebohm, N.; Lehmkuhl, K.; Schepmann, D.; Ametamey, S. M.; Seebohm, G.; Schmidt, T. J.; Wünsch, B. Synthesis and Pharmacological Evaluation of Enantiomerically Pure GluN2B Selective NMDA Receptor Antagonists. *ChemMedChem* **2018**, *13* (15), 1580−1587.
(41) Hübner, H.; Haubmann, C.; Utz, W.; Gmeiner, P. Conjugated Enynes as Nonaromatic Catechol Bioisosteres: Synthesis, Binding Experiments, and Computational Studies of Novel Dopamine Receptor Agonists Recognizing Preferentially the D3 Subtype. *J. Med. Chem.* **2000**, *43* (4), 756−762.
(42) Liu, H.; Hofmann, J.; Fish, I.; Schaake, B.; Eitel, K.; Bartuschat, A.; Kaindl, J.; Rampp, H.; Banerjee, A.; Hübner, H.; Clark, M. J.; Vincent, S. G.; Fisher, J. T.; Heinrich, M. R.; Hirata, K.; Liu, X.; Sunahara, R. K.; Shoichet, B. K.; Kobilka, B. K.; Gmeiner, P. Structure-Guided Development of Selective M3 Muscarinic Acetylcholine Receptor Antagonists. *Proc. Natl. Acad. Sci. U. S. A.* **2018**, *115* (47), 12046−12050.
(43) Hasebein, P.; Frehland, B.; Lehmkuhl, K.; Fröhlich, R.; Schepmann, D.; Wünsch, B. Synthesis and Pharmacological

Evaluation of Like- and Unlike-Configured Tetrahydro-2-Benzazepines with the α-Substituted Benzyl Moiety in the 5-Position. *Org. Biomol. Chem.* **2014**, *12* (29), 5407−5426.
(44) Miyata, K.; Schepmann, D.; Wünsch, B. Synthesis and σ Receptor Affinity of Regioisomeric Spirocyclic Furopyridines. *Eur. J. Med. Chem.* **2014**, *83*, 709−716.
(45) Meyer, C.; Neue, B.; Schepmann, D.; Yanagisawa, S.; Yamaguchi, J.; Würthwein, E. U.; Itami, K.; Wünsch, B. Improvement of Σ1 Receptor Affinity by Late-Stage C-H-Bond Arylation of Spirocyclic Lactones. *Bioorg. Med. Chem.* **2013**, *21* (7), 1844−1856.
(46) Shingala, J. R.; Balaraman, R. Antihypertensive Effect of 5-HT1A Agonist Buspirone and 5-HT2B Antagonists in Experimentally Induced Hypertension in Rats. *Pharmacology* **2005**, *73* (3), 129−139.
(47) Edagawa, Y.; Saito, H.; Abe, K. Stimulation of the 5-HT(1A) Receptor Selectively Suppresses NMDA Receptor-Mediated Synaptic Excitation in the Rat Visual Cortex. *Brain Res.* **1999**, *827* (1−2), 225−228.
(48) Yuen, E. Y.; Jiang, Q.; Chen, P.; Gu, Z.; Feng, J.; Yan, Z. Serotonin 5-HT1A Receptors Regulate NMDA Receptor Channels through a Microtubule-Dependent Mechanism. *J. Neurosci.* **2005**, *25* (23), 5488−5501.
(49) Yuen, E. Y.; Jiang, Q.; Chen, P.; Feng, J.; Yan, Z. Activation of 5-HT2A/C Receptors Counteracts 5-HT1A Regulation of N-Methyl-D-Aspartate Receptor Channels in Pyramidal Neurons of Prefrontal Cortex. *J. Biol. Chem.* **2008**, *283* (25), 17194−17204.
(50) Woods, S.; Clarke, N.; Layfield, R.; Fone, K. 5-HT6 Receptor Agonists and Antagonists Enhance Learning and Memory in a Conditioned Emotion Response Paradigm by Modulation of Cholinergic and Glutamatergic Mechanisms. *Br. J. Pharmacol.* **2012**, *167* (2), 436−449.
(51) Vasefi, M. S.; Yang, K.; Li, J.; Kruk, J. S.; Heikkila, J. J.; Jackson, M. F.; Macdonald, J. F.; Beazely, M. A. Acute 5-HT7 Receptor Activation Increases NMDA-Evoked Currents and Differentially Alters NMDA Receptor Subunit Phosphorylation and Trafficking in Hippocampal Neurons. *Mol. Brain* **2013**, *6* (1), 24.
(52) Hashimoto, K.; Sasaki, T.; Kishimoto, A. Old Drug Ifenprodil, New Hope for PTSD with a History of Childhood Abuse. *Psychopharmacology (Berl).* **2013**, *227* (2), 375−376.
(53) Temme, L.; Frehland, B.; Schepmann, D.; Robaa, D.; Sippl, W.; Wünsch, B. Hydroxymethyl Bioisosteres of Phenolic GluN2B-Selective NMDA Receptor Antagonists: Design, Synthesis and Pharmacological Evaluation. *Eur. J. Med. Chem.* **2018**, *144*, 672−681.

https://dx.doi.org/10.1021/acs.jmedchem.0c01912
J. Med. Chem. 2021, 64, 1170−1179